JOURNAL OF APPLIED PHYSICS VOLUME 95, NUMBER 11 1 JUNE 2004

Micromagnetics Pieter Visscher, Chairman

Micromagnetic simulation of ferromagnetic part-spherical particles

Richard P. Boardman, Hans Fangohr,[a] and Simon J. Cox
Computational Engineering and Design Group, School of Engineering Sciences, University of Southampton, Hampshire SO17 1BJ, United Kingdom

Alexander V. Goncharov, Alexander A. Zhukov, and Peter A. J. de Groot
School of Physics and Astronomy, University of Southampton, Hampshire SO17 1BJ, United Kingdom

(Presented on 8 January 2004)

The paramagnetic size limit for current magnetic storage media, particularly in sputtered grain storage, is being approached rapidly. To further increase media storage density, patterned media can be used which only need a single grain to store one bit of data. Chemical self-assembly techniques offer cost-effective methods to create templates, from which periodic arrays of magnetic structures can be formed. In contrast to systems of dots prepared by standard lithography, which have a cylindrical shape, dots prepared by chemical self-assembly template techniques are often spherical or part spherical in shape. In this article, we investigate the properties of such magnetic shapes using micromagnetic simulations. To represent accurately the geometry produced through chemical self-assembly methods, we attach a partial sphere (lower part) to a small ellipsoidal dome. We compute the hysteresis loops for various dot sizes and compare them with experimental results. In those below a critical diameter (140 nm in nickel), the hysteresis loop is square-like, resembling the uniform rotation of magnetization once the critical field is exceeded. For larger sizes, the hysteresis loop reverses reversibly around zero applied field but shows minor loops, placed symmetrically at the onset of magnetization reversal. These correspond to vortices penetrating and exiting the structure. In summary, we find that the coercive field of the droplets becomes zero above a critical diameter where the magnetization reversal behavior changes from single domain-like to vortex-like. Our results agree with experimental measurements performed on such structures. © *2004 American Institute of Physics.* [DOI: 10.1063/1.1688639]

INTRODUCTION

Current magnetic storage media types are approaching fundamental limits. The paramagnetic size limit for magnets causes those magnets which are below a particular size to become unstable at room temperature, capping their usefulness as long-term storage media. With traditional nonpatterned media created by sputtering this problem is becoming more critical, as these grains are reduced while pursuing greater bit density. Since many grains are used to represent a single bit in nonpatterned media, this severely limits the bit density that can be provided by this type of media.

One answer to this problem is to create patterned media which, by having a larger grain size, only need a single grain to store one bit of data; this then allows significant increase in the storage density of the media.

There are several different ways of creating patterned media. Photolithographic methods are limited down to half-micron sizes. Electron beam lithography is uneconomical when considered on a large scale.

Self-assembly methods appear to be a cost-effective way to create templates, from which an array of magnetic structures can be formed consisting of nanoclusters of atoms.[1] One particular method of chemical selfassembly involves the formation of templates through the evaporation of an aqueous suspension of polystyrene latex spheres,[2] initiating the self assembly. Using these spheres, it is possible to create magnetic structures from sizes of 50 nm by filling the spaces between the close-packed spheres with some material through electrochemical deposition. By etching away the polystyrene spheres, a template is formed. This template can then be filled with magnetic material, and by varying the fill amount of the resulting spherical holes, connected or disconnected arrays of dots can be formed.

Previous work has shown that flat circular nanomagnets exhibit single-domain magnetization reversal below a critical size and above this size will enter the vortex state around zero field.[3–5] In this work we investigate the behavior of disjunct objects for a fill height smaller than half of the diameter of the spheres (see Fig. 1).

We simulate droplets resulting from the partial filling of templates with spherical voids. The measurements from the base to the top of the droplets are approximately $3/7d$, d being the diameter of the overall bounding sphere; the droplet follows the bounding sphere for $2/7d$ and the remaining $1/7d$ section is ellipsoidal (see Fig. 1).

[a]Author to whom correspondence should be addressed.

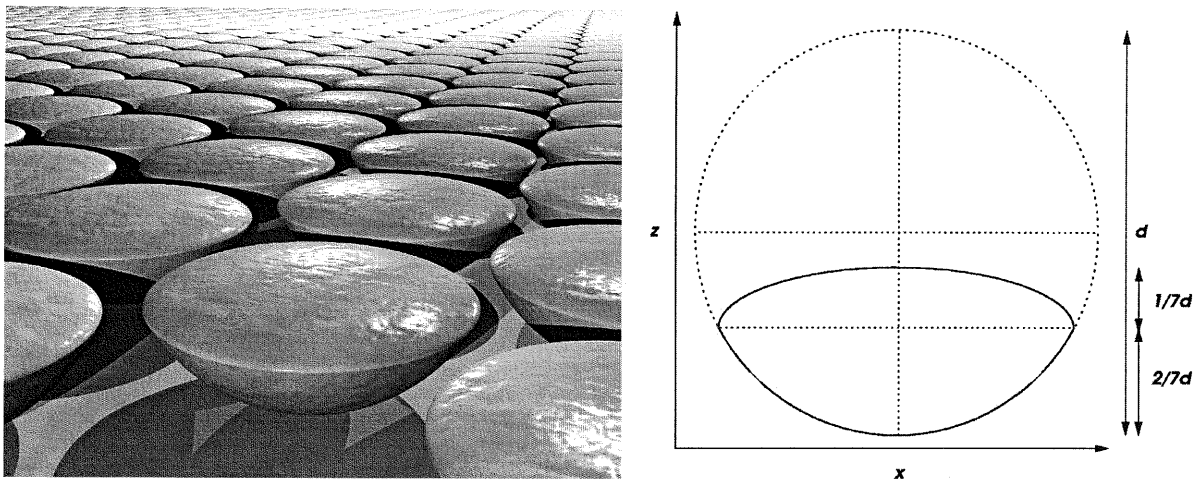

FIG. 1. (Left) An artist's impression of an array of "droplets" representing the rounded ellipsoidal upper and (right) a cross-sectional diagram in which the solid line shows the droplet shape in the $x-z$ plane.

METHOD

We use the object-oriented micromagnetic framework (OOMMF) software provided by the National Institute of Standards and Technology.[6] This software uses the Landau–Lifshitz–Gilbert equation[7]

$$\frac{d\mathbf{M}}{dt} = -|\bar{\gamma}|\mathbf{M}\times\mathbf{H}_{\text{eff}} - \frac{|\bar{\gamma}|\alpha}{M_s}\mathbf{M}\times(\mathbf{M}\times\mathbf{H}_{\text{eff}}), \tag{1}$$

where $\mathbf{H}_{\text{eff}}$ is the magnetization (i.e., the magnetic moment per unit volume), $\mathbf{M}$ is the effective magnetic field, α is the Landau–Lifshitz phenomenological damping parameter, and $\bar{\gamma}$ is the electron gyromagnetic ratio.

We simulate nickel, a slightly anisotropic material with an exchange coupling constant A of 9×10^{-12} J/m, a magnetization M_s of 4.9×10^5 A/m. Comparative simulations show that the small anisotropy of nickel at room temperature does not affect the results presented in this work. We can calculate the exchange length for nickel from the equation $\sqrt{2A/\mu_0 M_s^2}$;[8] in this instance it is about 8 nm. This provides an indication of the necessary resolution of the numerical discretisation; if this granularity is unacceptably large, inaccuracies within the calculation arise associated with the angle between the magnetization in two adjacent discrete cells.[9] In these simulations we use a discrete cell size of 5 nm^3; halving this and repeating the simulation leaves the results virtually unaffected, indicating that it is not the finite difference discretisation which triggers the nucleation of the vortex.

Starting from an initially uniform magnetization state pointing in the x direction, we apply a high magnetic field capable of maintaining a homogeneous magnetization and reduce this field until the magnetization is reversed.

RESULTS

Figure 2 shows the hysteresis loop associated with a droplet of bounding sphere diameter d of 140 nm; inset with this loop are cross-sectional snapshots of the magnetization during the reduction of the applied field. Initially, the magnetization is homogeneous in the direction of the applied field (A). After reducing the field to approximately 25 mT there is a slight drop in the net magnetization; this is a precursor to vortex penetration. At around 15 mT, the homogeneous magnetization collapses into the vortex state (B). Reducing the applied field to zero results in the vortex shifting to the center (C) and further reduction causes the vortex to move away from the center (D). Finally, the applied field, now pointing in the negative x direction, forces the vortex out of the system, leaving the magnetization pointing homogeneously in the x direction. The cross-sectional cut planes show the states in the $x-y$ plane whilst the field is being reduced.

At high fields (i.e., where $|\mathbf{B}|\geqslant 50$ mT) the Zeeman energy dominates and the magnetization is mainly aligned with this applied field. For small fields the vortex can move continuously in the system (insets B, C, and D in Fig. 2). This allows the overall magnetic moment to follow the applied field, resulting in a reversibly linear $\mathbf{B}-\mathbf{M}$ characteristic around $|\mathbf{B}|=0$. There is an energy barrier for a vortex to penetrate, form and disappear, which results in the two symmetrically placed hysteresis loops at 15 mT$\leqslant|\mathbf{B}|\leqslant$50 mT. This hysteresis is similar to the behavior in large ($d=0.8$ μm) cylindrical dots but very different to dots of the

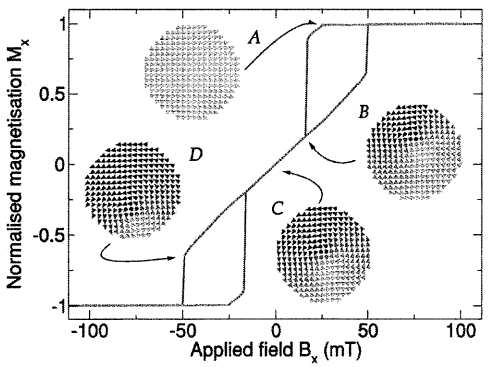

FIG. 2. Hysteresis loop with $x-y$ cut planes showing vortex propagation in a droplet with a bounding sphere diameter of $d=140$ nm.

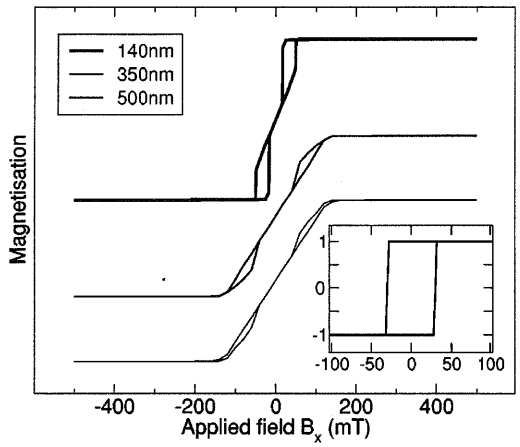

FIG. 3. Hysteresis loops for droplets of bounding sphere diameter 140, 350, and 500 nm; note that the loops are offset in the y direction for clarity. (Inset) The hysteresis loop for a droplet of bounding sphere diameter 50 nm.

same size order (for example, Refs. 10 and 11) which show square-like and nonreversible hysteresis loops.

The associated hysteresis curves resulting from the simulations of droplets with bounding sphere sizes of 140, 350, and 500 nm are shown in Fig. 3. From these, we can see that although the overall behavior in these three systems remains similar (i.e., vortex-like) there are slight changes in the shapes of the hysteresis loops indicating that there is some change in the nucleation and disappearance methods of the vortex. The vortex penetration for these large systems shows behavior which is related to that of spheres and will be described elsewhere.[11]

We have studied size dependence by performing micromagnetic simulations on droplets of bounding sphere size between 20 and 400 nm. From this study we find that apart from a slight minimisation of the demagnetisation energy at the extremeties, the droplets behave as single domains at 130 nm and below (see inset, Fig. 3), with a coercivity which increases as the bounding sphere diameter is reduced, and at 140 nm and above the behavior is vortex-like. Above this size, the coercive fields drop to zero as the droplets enter the vortex state. This is a significantly larger diameter than the value of 68 nm for nickel spheres (calculated from $r_c = \sqrt{(9A/\mu_0 M_s^2)}[\ln(2r_c/a)-1]$;[12] this figure also agrees with our simulations of spheres to within a few nm).[11]

Figure 4 compares simulation results for a droplet of bounding sphere size 500 nm with experimental results measured using a magneto-optical Kerr effect probe. A striking similarity can be seen between these results, particularly the vortex nucleation point (approximately 100 mT) and the narrow openings in the hysteresis loop (around 50 mT).

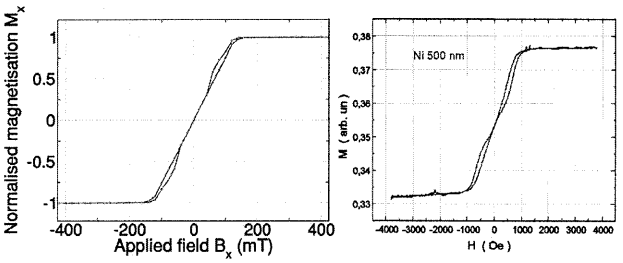

FIG. 4. Comparison between hysteresis loops from the simulation (left) and experimental measurement (right) of flat droplets with a bounding sphere diameter d of 500 nm.

SUMMARY

We have simulated the magnetization reversal in droplet nanodots, and we observe two different mechanisms for this reversal—the single-domain state and the vortex state.

If the overall size of the droplet system is increased then we notice a distinct transition from the single domain state to the vortex state, which we identify as being at a droplet bounding sphere radius of 140 nm (physical droplet diameter in this instance is around 90% of the bounding sphere radius, approximately 126 nm). This change occurs at a significantly smaller diameter than for thin circular nanodots.

The "soft" vortex behavior (i.e., it will readily adjust its position to accommodate a change in applied field) observed in the large droplets is a useful characteristic in sensor applications; smaller droplets have the square hysteresis loops desirable for data storage.

ACKNOWLEDGMENT

The authors acknowledge the support of the Wohlfarth Memorial Fund for this work.

[1] A. A. Zhukov, A. V. Goncharov, P. A. J. de Groot, P. N. Bartlett, and M. A. Ghanem J. Appl. Phys. **93**, 7322 (2003).
[2] P. N. Bartlett, J. J. Baumberg, P. R. Birkin, M. A. Ghanem, and M. C. Netti, Chem. Mater. **14**, 2199 (2002).
[3] R. P. Cowburn, D. K. Koltsov, A. O. Adeyeye, M. E. Welland, and D. M. Tricker, Phys. Rev. Lett. **83**, 1042 (1999).
[4] J. K. Ha, R. Hertel, and J. Kirschner, Phys. Rev. B **67**, 224432 (2003).
[5] L. D. Buda, I. L. Prejbeanu, U. Ebels, and K. Ounadjela, Comput. Mater. Sci. **24**, 181 (2002).
[6] M. J. Donahue and D. G. Porter, Interagency Report No. NISTIR 6376, National Institute of Standards and Technology, 1999.
[7] L. Landau and E. Lifshitz, Phys. Z. Sowjetunion **7**, 153 (1935).
[8] H. N. Bertram and C. Seberino, J. Magn. Magn. Mater. **193**, 388 (1999).
[9] M. J. Donahue and R. D. McMichael, Physica B **233**, 272 (1997).
[10] M. Schneider, H. Hoffmann, and J. Zweck, J. Magn. Magn. Mater. **257**, 1 (2002).
[11] R. P. Boardman and H. Fangohr (unpublished).
[12] R. C. O'Handley, *Modern Magnetic Materials* (Wiley Interscience, New York, 1999).